A PHYSICAL MECHANISM FOR ROTATING LINES OF SYMMETRY IN BWR OUT-OF-PHASE LIMIT CYCLE OSCILLATIONS

A. Wysocki*, A. Manera, T. Downar
University of Michigan
2355 Bonisteel Blvd, Ann Arbor, MI 48109
awysock@umich.edu; manera@umich.edu; downar@umich.edu

J. March-Leuba
Oak Ridge National Laboratory
P.O. Box 2008, Oak Ridge, TN 37831
marchleubaja@ornl.gov

ABSTRACT

Recent neutronic/thermal-hydraulic (TH) coupled numerical simulations using full-core TRACE/PARCS and SIMULATE-3K BWR models have shown evidence of a specific "rotating mode" behavior (steady rotation of the symmetry line) in out-of-phase limit cycle oscillations, regardless of initial conditions and even if the first two azimuthal modes have different natural frequencies. The goal of the present work is to understand why the rotating mode is specifically preferred, and to determine under what conditions it might occur. This was accomplished using a multi-channel, multi-modal reduced-order model, using a special modification of the fixed pressure drop boundary condition to destabilize the out-of-phase mode over the in-phase mode. The four-channel model showed a clear preference for rotating mode behavior under standalone TH conditions and for conditions with weak neutronic feedback. When neutronic feedback was strengthened, the side-to-side mode (stationary symmetry line) was favored instead. A physical explanation has been put forth to explain why the rotating symmetry line behavior is preferred from a TH standpoint, demonstrating that the system is most unstable when the variation in the total inlet flow rate is minimized, and that the rotating mode is the most successful in minimizing this variation as compared to the side-to-side case or any other oscillation pattern. An explanation for why the neutronic channel coupling appears to favor a stationary symmetry line rather than a rotating symmetry line is left as a topic of future investigation.

KEYWORDS
BWR stability, limit cycle, rotating mode, time domain analysis

1. INTRODUCTION

Out-of-phase oscillations in boiling water reactors (BWRs) can be examined as a superposition of the first two azimuthal modes of the static neutron flux. A "side-to-side" out-of-phase behavior (stationary symmetry line) can occur when the azimuthal modes oscillate with the same phase shift; a "rotating" out-of-phase behavior (steady rotation of the symmetry line) occurs when the phase shift between modes is 90° [1] [2]. Typically, it has been assumed that the phase shift between modes is arbitrary, depending only on initial conditions and the natural frequencies of each azimuthal mode separately; however, a recent study by Wysocki et al. [3] using the TRACE/PARCS coupled code system, and an additional study by Dokhane et al. [4] using the SIMULATE-3K code, found a specific tendency towards the rotating pattern under asymptotic limit cycle conditions for at least some out-of-phase full-core simulation conditions. The phase shift between modes remained at roughly 90° in the limit cycle even though the

natural frequency of each azimuthal mode differed; this suggested a nonlinear coupling mechanism between modes promoting the specific 90° (rotating) behavior.

The primary focus of the current study is to provide a physical explanation for why the rotating mode limit cycle behavior might be favored over the side-to-side mode, and under what conditions this is true. To that end, the scope has been narrowed to smaller "*N*-channel" models including either $N = 2$ or $N = 4$ channels, rather than a full-core model. Primarily, the four-channel model will be used, as this gives the fewest number of channels while still allowing for two separate azimuthal modes (in the coupled case). In addition, a reduced-order model (ROM) is used, which provides a variety of advantages in simplifying the analysis and allowing for ease of physical insights. From this simplified model, insights have been gained into the physical causes for the oscillatory behavior, e.g. rotating versus side-to-side, and these insights may be easily extended for an understanding of the full-core results shown in the previous works.

A secondary aim of the current study is to present a new approach for boundary condition treatment in multi-channel systems which, to the author's knowledge, has not been done previously in quite the same way. This approach freely allows the user to control the preferred oscillation type (in-phase versus out-of-phase) by simple adjustment of inlet and outlet plena loss factors, while maintaining consistency across cases for clear comparison if done properly.

Previous authors have examined, both experimentally and theoretically, the behavior of systems of N identical TH channels connected in parallel via common inlet and outlet plena, in particular when the total flow rate among channels is held constant. For $N = 2$, only the $(0°, 180°)$ pattern is possible (i.e. phase shift of $180°$ between the individual channel oscillations). For $N = 4$, Nakanishi [5] reported experimental results in which two pairs of channels form, with the two channels of each pair oscillating counter-phase to each other but with an arbitrary phase shift for one pair relative to the other. This can be expressed as $(0°, \phi, 180°, 180° + \phi)$, where ϕ is the arbitrary phase shift between the two pairs.

This is sufficient to ensure that the total flow rate remains constant in the linear case (i.e. perfectly sinusoidal oscillations); however, the authors could find no examples in which the nonlinear oscillation case (i.e. oscillations with additional Fourier frequency components) was analyzed, either theoretically or for large-amplitude TH oscillations. As will be shown in this paper, the additional nonlinear terms make a difference in how well the variation in total flow rate is minimized in the rotating mode case versus the side-to-side mode case; this fact, as will be argued in this paper, leads to a condition in which the rotating mode is specifically favored over the side-to-side mode, with both numerical results and physical explanations provided to support the claim.

2. METHODOLOGY

2.1. Reduced-Order Model

The ROM used in the present study was introduced by Karve et al. [6], and was selected here as being perhaps the simplest model available which still includes all the elements needed for this study. The original model described consists of a single thermal-hydraulic channel with fuel temperature and coolant density feedback provided via a point kinetics model for neutronics. A description of the phase variables solved for in the present study is given in Table I; these are identical to the phase variables in the original model except that the model has been extended to allow for multiple thermal hydraulic channels in parallel, connected via common inlet and outlet plena. In addition, an option has been added to employ higher-order modal kinetics, up to the first three neutronic modes (*i.e.* the fundamental and first two azimuthal neutronic modes).

Table I. Description of phase variables solved for in the model as implemented in the current work

Variable	Description
$\mu_i(t)$	Axial location of boiling boundary for channel i
$s_i(t)$	Slope of quality in two-phase region for channel i
$v_i(t)$	Inlet velocity for channel i
$T_{1,1\phi,i}(t)$	kth expansion coefficient for fuel temperature in single-phase region for channel i
$T_{1,2\phi,i}(t)$	kth expansion coefficient for fuel temperature in two-phase region for channel i
$n_m(t)$	Neutron density for neutronic mode m
$c_m(t)$	Neutron precursor concentration for neutronic mode m

To accomplish these changes, the equations and phase variables governing thermal hydraulics and fuel heat conduction were trivially extended to N channels, with each channel i being solved independently in complete analogy to the original single-channel treatment, with two exceptions: the conduction solution was reduced to a single-region problem (in the radial direction) for simplicity, and the inlet and outlet k-factor treatment was altered in a way that was unique to the multi-channel system, as discussed in the next section. In addition, the neutron kinetics treatment was extended from simple point kinetics to multimodal kinetics, allowing for any number of neutronic modes M as specified by the user.

The resulting system consists of $(5N + 2M)$ nonlinear ODEs, with phase variables given in Table I, which were solved using MATLAB's built-in *ode23* function, a one-step second-order Runge Kutta method. One additional detail to note in the current implementation was the use of a simple limiter which set any negative values for the phase variables to zero at each solution step, preventing negative solutions which (due to the assumptions inherent in the equations) led to runaway divergence of the solution to infinity in either direction. This proved necessary for the problems shown in this study, as the limit cycles often had large enough amplitudes to give negative velocities during a portion of the oscillation period.

The reader is referred to the original paper by Karve et al. [6] for a detailed description of the underlying fluid and fuel heat conduction equations. For the multi-modal kinetics equations, the reader is referred to other sources, such as Dokhane [7], from which the current implementation was directly adapted.

2.2 Boundary Condition Treatment and Inlet Plenum Loss Factors

The behavior of a system of parallel flow channels undergoing oscillations (most commonly, density-wave oscillations) has been the topic of numerous studies, both experimental and analytical. Boundary conditions play an important role in determining the stability characteristics, *e.g.* whether the in-phase or out-of-phase oscillation mode dominates. For the case of in-phase oscillations, the recirculation loop dynamics play a role, and the boundary conditions may reflect this in terms of additional pressure drop terms or other treatment. However, for the case of out-of-phase oscillations, Grandi et al. [8] have shown that recirculation loop dynamics play virtually no role at all, and the results are almost identical if one eliminates the recirculation loop dynamics from the model and imposes a constant total core inlet flow rate and a constant core pressure drop boundary condition instead.

More recently, Munoz-Cobo et al. [8] have argued that a constant pressure drop boundary condition should not be imposed along with a constant total mass flow rate condition, as this leads to an overdetermined system of equations and artificially inhibits the variations in total inlet flow rate.

Alternately, Dokhane [7] was able to impose a fixed pressure drop boundary condition and still obtain in-phase oscillations, provided that the oscillations remained small in amplitude (1%).

As will be demonstrated in the Results section, applying a fixed pressure drop boundary condition from only the inlet to the outlet of each channel prevents any coupling between channels, at least when neutronics are disabled. In a real BWR, though, the channels are coupled thermal-hydraulically through the inlet and outlet plena, which has a flow rate equal to the sum of the flow rates in all channels at the channel inlet and outlet, respectively. By including a pressure drop term which operates on the total core flow rate, a mechanism is created by which the channels may be coupled to each other. The effects of this extra loss term on the stability characteristics of the system, and the physical reason why it promotes either out-of-phase or in-phase behavior (depending on the values chosen), will be described in detail in the Results section.

In the present work, the pressure loss for the inlet plenum is termed $\Delta P_{below}(t)$ and is applied as a concentrated pressure loss with a local loss factor k_{below} as given by

$$\Delta P_{below}(t) = k_{below}\rho_l v_{inlet,avg}^2(t)\,, \tag{1}$$

where ρ_l is the single-phase liquid density, and $v_{in,avg}(t)$ is the time-dependent average inlet velocity given by

$$v_{inlet,avg}(t) = \frac{1}{N}\sum_{i=1}^{N} v_i(t)\,, \tag{2}$$

where N is the total number of channels and $v_i(t)$ is the inlet velocity for channel i. Likewise, an additional term $\Delta P_{above}(t)$ can be derived based on the average outlet velocity across all channels, properly weighted by channel outlet densities (based on void fraction). This has been done in a more thorough work by Wysocki [9]; however, such an analysis is omitted in the present work, for brevity.

Note that a separate loss term $\Delta P_{inlet,i}(t)$ is still included in the model (as originally implemented by Karve et al.), and operates on the inlet velocity of <u>each channel</u> separately. Namely,

$$\Delta P_{inlet,i}(t) = k_{inlet}\rho_l v_i^2(t)\,. \tag{3}$$

Therefore, for example, if one wishes to increase $\Delta P_{below}(t)$ from its default value of 0.0 to some positive value, one may also decrease $\Delta P_{inlet}(t)$ by the same amount in order to maintain precisely the same overall ΔP_{tot} throughout the model, thus maintaining the same steady-state conditions as well. This is an attractive feature which allows for true "apples-to-apples" comparison between cases.

All calculations performed in this paper were done with MATLAB, including use of the MATLAB Symbolic Toolbox for calculation of eigenvalues and eigenvectors for the linearized system (*i.e.* the Jacobian) around the steady-state values for the original system of nonlinear ODEs. This was used to provide further insights into the results.

3. RESULTS

3.1. Initial Coupled Results

Table II shows the steady-state values calculated for the single-channel model, named Case C-1A, with $N_{sub} = 1.5$ and $\tilde{n} = 1.69$. These values correspond exactly to the values calculated by Karve et al. [6] for the same conditions. The leading eigenvalue for this case was found to belong to the complex pair

$0.263 \pm 7.840i$, which in the time domain corresponds to a growing exponential based on the real part multiplied by a sinusoidal oscillation with frequency based on the complex part.

Table II. Steady-state values for all phase variables in all channels, across all cases shown in this paper, for $N_{sub} = 1.5$

Variable	Steady-state value
$\tilde{\mu}$	0.231
$\tilde{s}$	0.350
$\tilde{v}$	0.878
$\tilde{n}$	1.69
$\tilde{c}$	2957

However, initially, standalone TH cases were desired; to accomplish this, all parameters were kept the same (including $\tilde{n}$) except that the feedback reactivity coefficients c_1 and c_2 in the model (corresponding to void and fuel temperature feedback, respectively) were reduced from their original values of -0.15 and $-2.0x10^{-5}$, respectively (in nondimensional terms), to $c_1 = c_2 = 0.0$. Thus, changes in void fraction and fuel temperature have no effect on the reactivity terms, so that the power levels (and therefore the heat reaching the coolant) remain constant, acting as a fixed-heat-flux boundary condition typical of standalone TH problems.

This, however, decreased the oscillatory eigenvalue pair from $0.263 \pm 7.840i$ to $-4.275 \pm 5.852i$, bringing the operating point far within the stable region, due to the loss of the neutronic feedback which has a destabilizing effect. To compensate, the values of k_{inlet} and k_{outlet} in the TH momentum equation were adjusted to bring the standalone TH case back to slightly unstable conditions. In the original model by Karve et al., values of $k_{inlet} = 15$ and $k_{outlet} = 2.5$ were given; for standalone TH cases in the current study, values of $k_{inlet} = 2.8$ and $k_{outlet} = 6.0$ were chosen instead. The methodology for choosing this values was based on maintaining the same ΔP_{tot} across the model while also giving the desired real eigenvalue component; further details are given in a separate work [9].

3.2. Standalone TH Results

3.2.1. Two-channel cases

Two different two-channel standalone TH cases were run: Case S-2A, using values of $k_{inlet} = 2.8$ and $k_{below} = 0.0$, and Case S-2B, using values of $k_{inlet} = 1.8$, and $k_{below} = 1.0$. Eigenvalues are shown in Table III. Note that each eigenvalue (or complex eigenvalue pair) is repeated, occurring once per channel, with each eigenvalue matching those for a separate single-channel case that was also performed (not shown here). Time-dependent channel inlet velocity values as well as the phase shift between the velocity oscillations in each channel are shown in Figure 1 and Figure 2. To find the phase shift values, a subroutine was used which finds all points for each channel velocity signal where the velocity crosses from below the steady state value to above that value (linearly interpolating the nearest two time points in the signal), then comparing that "crossover point" to the most recent crossover point for Channel 1, finding the time difference as a fraction of the total oscillation period then multiplying by 360 degrees to find the phase shift value at that point in time. All such phase shift values were then plotted consecutively as a single timeseries with phase shift on the y-axis.

Table III. Eigenvalues and corresponding oscillation types for the two-channel standalone TH case with $k_{inlet} = 2.8$ and $k_{below} = 0.0$ (Case S-2A), or with $k_{inlet} = 1.8$ and $k_{below} = 1.0$ (Case S-2B)

Case S-2A		Case S-2B	
Eigenvalue	**Oscillation Type**	**Eigenvalue**	**Oscillation Type**
0.330+8.277i	Arbitrary	0.843-8.290i	Out-of-phase
0.330+8.277i	Arbitrary	0.843+8.290i	Out-of-phase
0.330-8.277i	Arbitrary	0.330+8.277i	In-phase
0.330-8.277i	Arbitrary	0.330-8.277i	In-phase
0.000	-	0.000	-
0.000	-	0.000	-
-0.300	-	-0.300	-
-0.300	-	-0.300	-
-0.315	-	-0.315	-
-0.315	-	-0.315	-
-47.211	-	-44.772	-
-47.211	-	-47.211	-
-199.889	-	-199.889	-
-199.889	-	-199.889	-

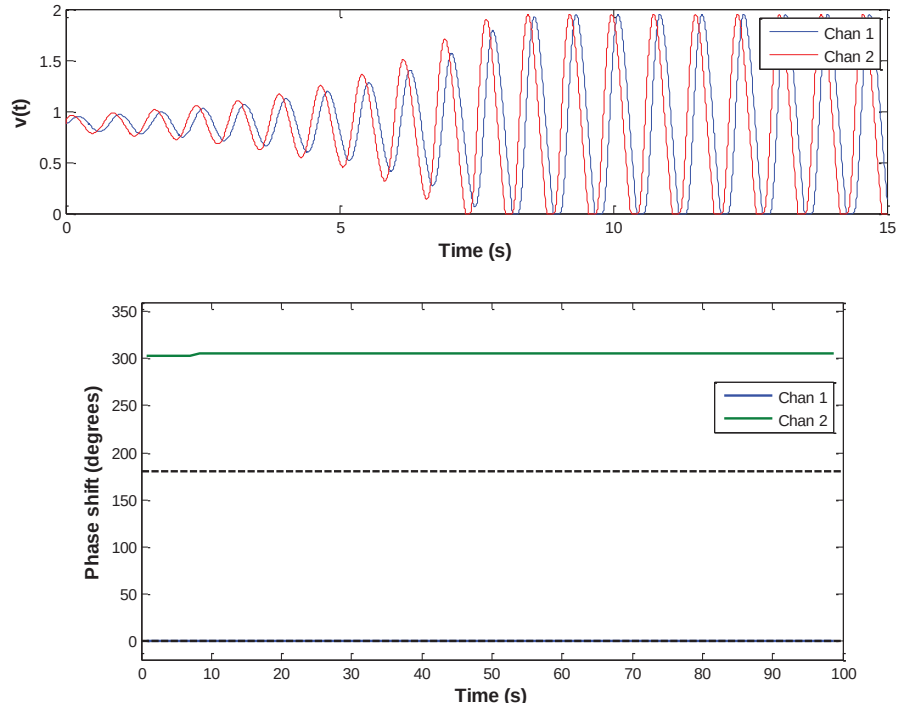

Figure 1. Inlet velocity $v_i(t)$ for each channel i (top) and evolution over time of the phase shift of each channel relative to Channel 1 (bottom), for the two-channel standalone TH case with $k_{inlet} = 2.8$ and $k_{below} = 0.0$ (Case S-2A).

The final (asymptotic) phase shift between channels shown in Figure 1 is arbitrary; different cases were also performed with different initial conditions, leading to different final phase shift values. This is because the fixed ΔP_{tot} boundary condition is applied to each channel separately, with all ΔP terms operating on individual channel parameters only. Likewise, in Table III the first two eigenvalue pairs of $0.330 \pm 8.277i$ are degenerate, meaning that they have the same eigenvalues and the eigenvectors can occur in any point in the corresponding two-dimensional vector space and need not be orthogonal; *i.e.* they correspond neither to out-of-phase nor in-phase oscillations *per se*, but rather can be chosen arbitrarily (in terms of phase shift between channels).

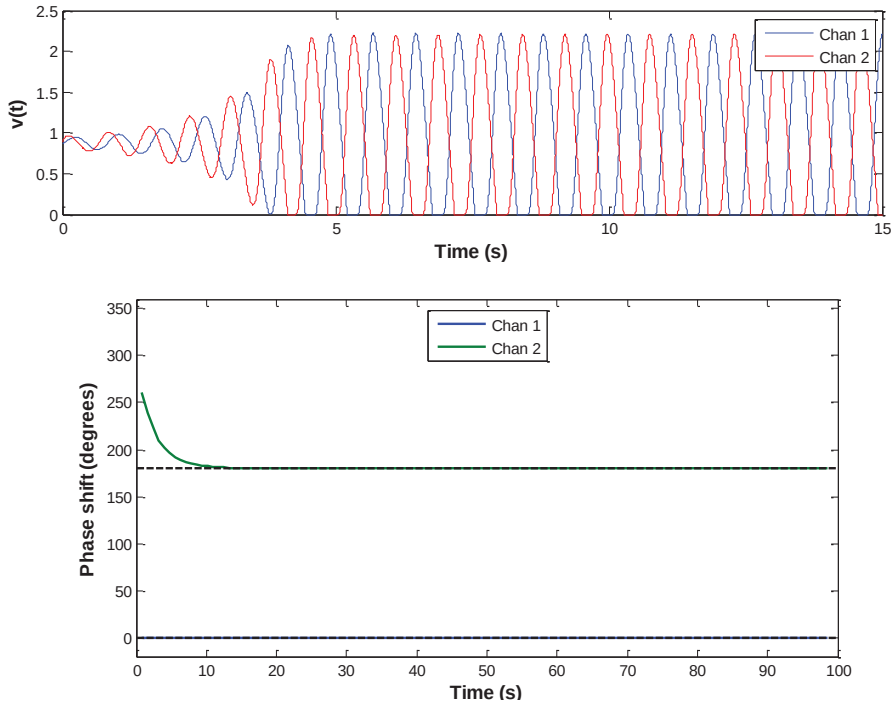

Figure 2. . Inlet velocity $v_i(t)$ for each channel i (top) and evolution over time of the phase shift of each channel relative to Channel 1 (bottom), for the two-channel standalone TH case with $k_{inlet} = 1.8$ and $k_{below} = 1.0$ (Case S-2B).

In order to obtain a distinct in-phase or out-of-phase characteristic behavior, the k_{below} term must be nonzero in this implementation. This is seen in Case S-2B (Figure 2), which shows a clear evolution towards out-of-phase oscillation (*i.e.* 180° phase shift between channels), regardless of initial conditions. This is represented also in Table III, which indicates that one complex eigenvalue pair still exists at the same value of $0.330 \pm 8.277i$, but now the other pair exists at $0.843 \pm 8.290i$ instead. Inspection of the corresponding eigenvector reveals that this corresponds to an out-of-phase oscillation case (180° phase shift between channels), while the $0.330 \pm 8.277i$ now corresponds specifically to in-phase oscillations (0° phase shift).

The physical reason for this behavior in Case S-2B is as follows. In the in-phase oscillation case, the average inlet velocity ($v_{inlet,avg}(t)$ in Eq. (1)) oscillates identically to $v_1(t)$ and $v_2(t)$ (the individual channel velocities). Thus, the in-phase oscillation mode exhibits the exact same behavior as if two channels were independent (as in Case S-2A) or as in a corresponding single-channel case if it were performed instead. However, in the out-of-phase oscillation case, $v_{inlet,avg}(t)$ no longer oscillates the same as $v_1(t)$ and $v_2(t)$; in fact, $v_{inlet,avg}(t)$ is constant in time since the oscillation in channel 1 cancels out the oscillation in channel 2, at least for linear oscillations (for nonlinear oscillations with additional

Fourier frequency components, the average flow cannot in general be strictly constant). This means that $\Delta P_{below}(t)$ remains constant in time, meaning that each channel is effectively oscillating at a reduced total ΔP (since the contribution normally associated with $\Delta P_{below}(t)$ no longer "participates" in the oscillations).

More specifically, the effective pressure drop in the single-phase region is reduced (in terms of what oscillates), meaning that the effective two-phase to single-phase pressure drop ratio is increased. This, as is well known in the study of density-wave oscillations, has a destabilizing effect on the system, accounting for the increased real eigenvalue component of the out-of-phase mode shown in Table III.

It is significant to note that additional cases were performed by Wysocki [9], finding that the addition of an outlet plenum loss factor k_{above} had the opposite effect, promoting the in-phase mode over the out-of-phase mode, for the reverse reasoning as given above[1].

3.2.2. Four-channel cases

A four-channel case S-4B, in complete analogy to case S-2B, was performed, with $k_{below} = 1.0$ and $k_{inlet} = 1.8$. The eigenvalues (and eigenvectors) were simply repeats of the two-channel values, except with four complex pairs, one of which was the in-phase $0.330 \pm 8.277i$ pair and the other three of which were out-of-phase $0.843 \pm 8.290i$ pairs. This is expected, as there were now additional "degrees of freedom" in which the channels could oscillate out-of-phase in different combinations and still maintain a constant total inlet velocity (at least for the case of linear oscillations).

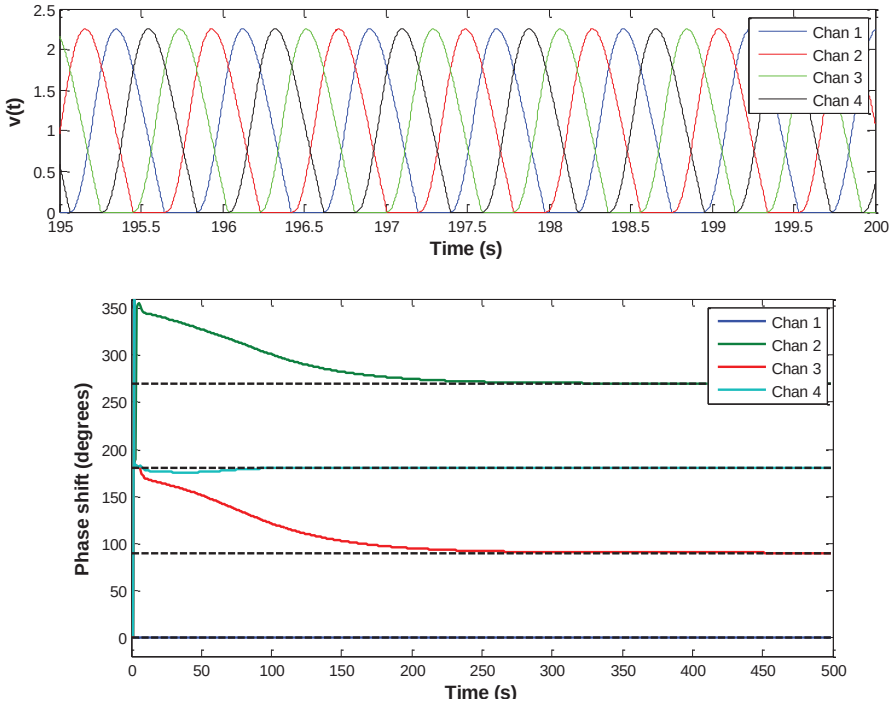

Figure 3. Inlet velocity $v_i(t)$ for each channel i (top) and evolution over time of the phase shift of each channel relative to Channel 1 (bottom), for the four-channel standalone TH case with $k_{inlet} = 1.8$ and $k_{below} = 1.0$ (Case S-4B).

[1] Furthermore, a negative value of k_{below} (or negative k_{above}) promoted the in-phase mode (or out-of-phase mode, respectively) as well, although the use of negative loss factors was purely academic and not physical.

Results of the numerical simulation are shown in Figure 3. As discussed in the Introduction, in the four-channel case the tendency is to form two pairs of counter-oscillating channels, with some (supposedly) arbitrary phase shift ϕ between the two pairs of channels. This is shown in the figure, in which Channels 1 and 4 quickly form into a 180° pair, and Channels 2 and 3 forming a separate 180° pair, starting from 10 seconds into the simulation and continuing indefinitely. However, the key finding is that the value of ϕ gradually moves towards 90.00° and remains there asymptotically; in other words, the four-channel model specifically favors the $(0°, 90°, 180°, 270°)$ oscillation pattern (to an arbitrary number of decimal places over time). This oscillation pattern naturally corresponds to a "rotating mode" behavior, except that the actual ordering of the channels is arbitrary for the standalone TH case. For the coupled case, the ordering is no longer arbitrary, and the behavior even more closely resembles that of the full-core rotating mode system, as will be shown in the next section.

One now wishes to understand why the $\phi = 90°$ behavior (i.e. "rotating mode") is favored, as opposed to $\phi = 180°$ ("side-to-side mode") or other patterns, for its significance on possible full-core BWR out-of-phase behavior. In fact, the reason for the rotating mode behavior can be understood by considering the average (or total) inlet flow rate among channels. Recall from the previous study on Case S-2B that a standalone TH system with a positive value for k_{below} will have an out-of-phase mode as the dominant oscillation mode[2], since the effective two-phase to single-phase pressure drop ratio is maximized when the average inlet flow rate is as close to constant as possible.

As discussed in the Introduction, the two pairs of counter-oscillating channels are sufficient to ensure a constant total flow rate in the linear oscillation case; however, especially for limit cycles, higher-frequency Fourier components exist in the velocity time signal, and this means that the average flow rate cannot be strictly constant regardless of phase shifts between channels.

In fact, the rotating mode is the specific pattern that is best at eliminating these higher frequency components from the average velocity signal. This will be shown by decomposing a representative inlet velocity signal from a particular channel during the limit cycle for Case S-4B; the original signal and the amplitude of each Fourier mode are shown in Figure 4. These were calculated using the eight-order Fourier expansion given by

$$f_1(t) = a_0 + \sum_{n=1}^{8} (a_n \cos(\omega n t) + b_n \sin(\omega n t)) \,, \tag{4}$$

where $f_1(t)$ is the original time signal and a_n, b_n, and ω are fitting parameters. The overall mode amplitude of each mode n, as given in Figure 4, is defined as

$$A_n = \sqrt{a_n^2 + b_n^2} \,. \tag{5}$$

Now the task is to analyze the average velocity signal when multiple identical channel signals are combined with various phase shifts. To do this, define

$$g(t) = \frac{1}{N} \sum_{i=1}^{N} f_i(t) \tag{6}$$

[2] Alternatively, k_{above} could be positive but sufficiently smaller than k_{below}. However, we will restrict our consideration the the case of $k_{above} = 0$ for the present discussion, for simplicity, as both cases yield the same conclusion.

where $g(t)$ is the average inlet velocity and N is the number of channels. First, consider the case of two identical channels with an arbitrary phase shift ϕ_2 between the channels. Using the expression for $f_1(t)$ in Eq. (4) with a frequency of ω, the expression for $f_2(t)$ is then simply

$$f_2(t) = f_1\left(t + \frac{\phi_2}{\omega}\right) \tag{7}$$

which can be substituted into Eq. (4) to find an explicit expression for $f_2(t)$ in terms of a summation of sine and cosine functions and the unknown quantity ϕ_2. Plugging the expressions for $f_1(t)$ and $f_2(t)$ into Eq. (6), one finds that the average flow rate between the two channels is given by

$$g(t) = a_0 + \sum_{n=1}^{8} \cos\left(\frac{n\phi_2}{2}\right)\left[a_n \cos\left(\omega n t + \frac{n\phi_2}{2}\right) + b_n \sin\left(\omega n t + \frac{n\phi_2}{2}\right)\right] \tag{8}$$

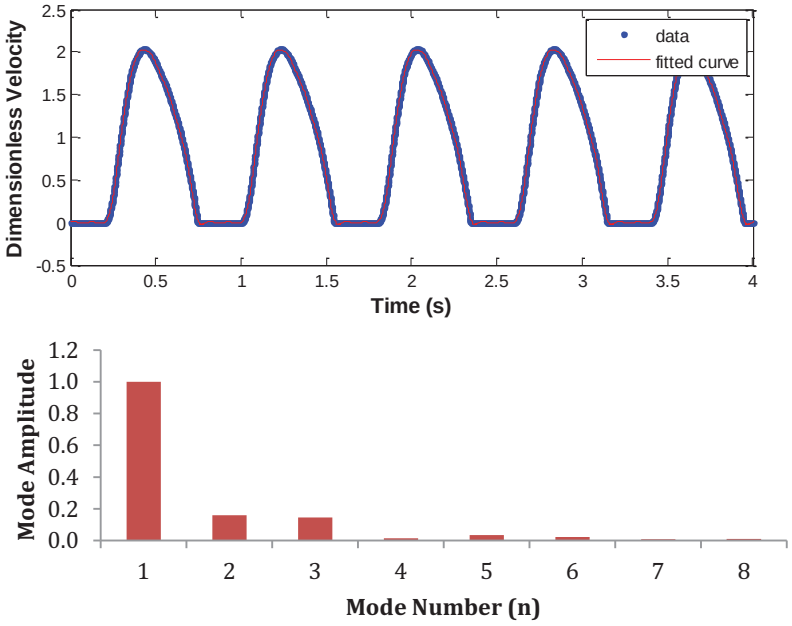

Figure 4. Inlet velocity signal for Channel 1 during the limit cycle for Case S-2B, along with the 8th-order Fourier curve fit (top), and the amplitude of each frequency mode in this Fourier curve fit (bottom).

The case of $\phi_2 = 0°$ corresponds to an in-phase oscillation between the two channels, while $\phi_2 = 180°$ corresponds to out-of-phase oscillations. Note by inspection that the out-of-phase case cancels out all odd n components in $g(t)$, while having no effect on the even n components (*i.e.* returning the same values from the original single-channel case). Therefore, all components in the out-of-phase case are less than or equal to those in the in-phase case in magnitude, and so the resulting function $g(t)$ will experience smaller oscillations in the out-of-phase case. Most importantly, the large $n = 1$ component in the original signal (Figure 4) is eliminated entirely, which is the most important reason why the out-of-phase mode helps minimize the variation in the total flow rate.

For completeness, the degree of variation in the average inlet velocity signal (which one is attempting to minimize) will be quantified using three different norms: the L^1-norm, L^2-norm, and L^∞-norm of $(g(t) - \tilde{g})$, over a single oscillation period, where $\tilde{g}$ is the steady-state average flow rate (equal to a_0 in the Fourier expansion). These norms are defined as

$$\|g(t)-\tilde{g}\|_b = \left(\int_0^{2\pi/\omega} |g(t)-\tilde{g}|^b dt \right)^{\frac{1}{b}} \tag{9}$$

where $\|g(t)-\tilde{g}\|_b$ is the L^b-norm of $(g(t)-\tilde{g})$, and $(2\pi/\omega)$ is a single oscillation period. The values of these norms, as a function of ϕ_2, are shown in Figure 5. It is clear that $\phi_2 = 180°$ minimizes the variation in the average flow rate, hence is the most unstable configuration for the nonlinear oscillations of Case S-2B.

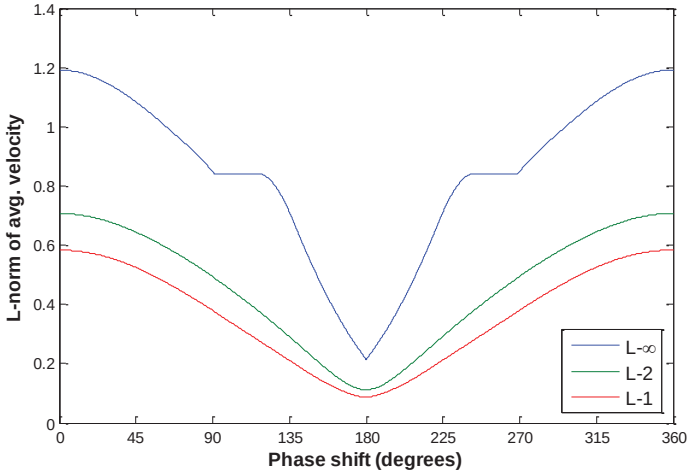

Figure 5. L-norms of the variation in average flow rate as a function of ϕ_2 over the range $(0°, 360°)$ for the two-channel case

The analysis will now be extended to the four-channel case, using $f_1(t)$ as given above as well as

$$f_2(t) = f_1\left(t + \frac{\phi}{\omega}\right), \tag{10}$$

$$f_3(t) = f_1\left(t + \frac{180°}{\omega}\right), \tag{11}$$

and

$$f_4(t) = f_1\left(t + \frac{\phi + 180°}{\omega}\right). \tag{12}$$

This assumes that $\phi_2 = 180°$, as concluded above for the most unstable case, and leaves ϕ as a free variable. This corresponds to the two pairs of counter-oscillating channels as described earlier.

The same analysis now yields

$$g(t) = \begin{cases} 0\ , & n \text{ odd} \\ a_0 + \sum_{n=1}^{8} \cos\left(\frac{n\phi}{2}\right)\left[a_n \cos\left(\omega n t + \frac{n\phi}{2}\right) + b_n \sin\left(\omega n t + \frac{n\phi}{2}\right)\right]\ . & n \text{ even} \end{cases} \tag{13}$$

By inspection, all odd modes are automatically zero, but also every $n = (2,6,10, \ldots)$ mode is also zero when $\phi = 90°$. This case, corresponding to the "rotating mode" with channel phase shifts of $(0°, 90°, 180°, 270°)$, results in the least possible variation in average flow rate, in terms of the L-norms shown in Figure 6.

It is expected, furthermore, that the rotating mode will minimize the variation in average flow rate (hence will be the most unstable mode) for any realistic limit cycle case (not just for the time signal analyzed here), due to most realistic oscillation patterns being dominated by the first three Fourier mode components ($n = 1,2,3$), all of which are eliminated completely by the rotating mode, leaving only the $n = 4$ mode and higher multiples of 4.

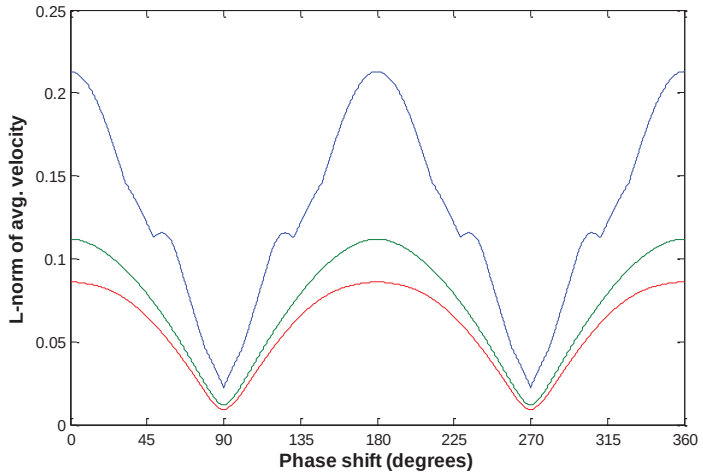

Figure 6. L-norms of the variation in average flow rate as a function of ϕ over the range $(0°, 360°)$ for the four-channel case, assuming $\phi_2 = 180°$

3.2. Coupled Results

This section describes results for the coupled neutronic-TH cases, in which the reactivity coefficients c_1 and c_2 were increased from 0.0 (standalone TH) to some fraction of their nominal values. First, with $c_1 = c_2 = 0.0$, the k_{inlet} and k_{outlet} values were returned to their nominal values of 15.0 and 2.5, respectively; then, k_{below} was increased until the out-of-phase modes had a real component of 1.000 (chosen arbitrarily, to yield sufficiently unstable results for quicker limit cycle evolution). Additional cases, shown in Table IV, were performed by incrementally decreasing k_{below} from this value, increasing c_1 and c_2 by the same fraction of their nominal amounts in order to maintain the same real component of 1.000 in the out-of-phase mode.

Table IV. Final limit cycle phase shift depending on the relative strength of neutronic versus TH channel coupling.

			Final Limit Cycle Phase Shift (degrees)			
Case	k_{below}	c_1, c_2 Multiplier	Chan. 1	Chan. 2	Chan. 3	Chan. 4
C-4A	11.000	0.388	0.0	0.0	180.0	180.0
C-4B	11.500	0.336	0.0	0.0	180.0	180.0
C-4C	11.750	0.310	0.0	0.0	180.0	180.0
C-4D	11.875	0.297	0.0	329.6	149.6	180.0
C-4E	12.000	0.284	0.0	318.1	138.1	180.0
C-4F	12.125	0.271	0.0	305.8	125.8	180.0
C-4G	12.250	0.258	0.0	270.0	90.0	180.0
C-4H	12.500	0.231	0.0	270.0	90.0	180.0
C-4I	13.000	0.177	0.0	270.0	90.0	180.0
C-4J	13.500	0.121	0.0	270.0	90.0	180.0

* The real component of the out-of-phase eigenvalue pair was 1.00000 in each case, the value of $\boldsymbol{k_{inlet}}$ was set to $(\mathbf{15.0} - \boldsymbol{k_{below}})$ in each case to maintain a constant total $\Delta \boldsymbol{P}$, and the steady-state solution was the same across all cases (as given in Table II).

Thus, a series of cases was created which had a progressively stronger neutronic coupling between channels (via c_1 and c_2) and a progressively weaker TH coupling between channels (via k_{below}). Results for the final limit cycle phase shift pattern for each case are shown in Table IV as well, with the phase shift plot examined visually in each case to ensure convergence (or run for a longer time if not). Phase shift as a function of time are shown in Figure 7 as well, for three select cases.

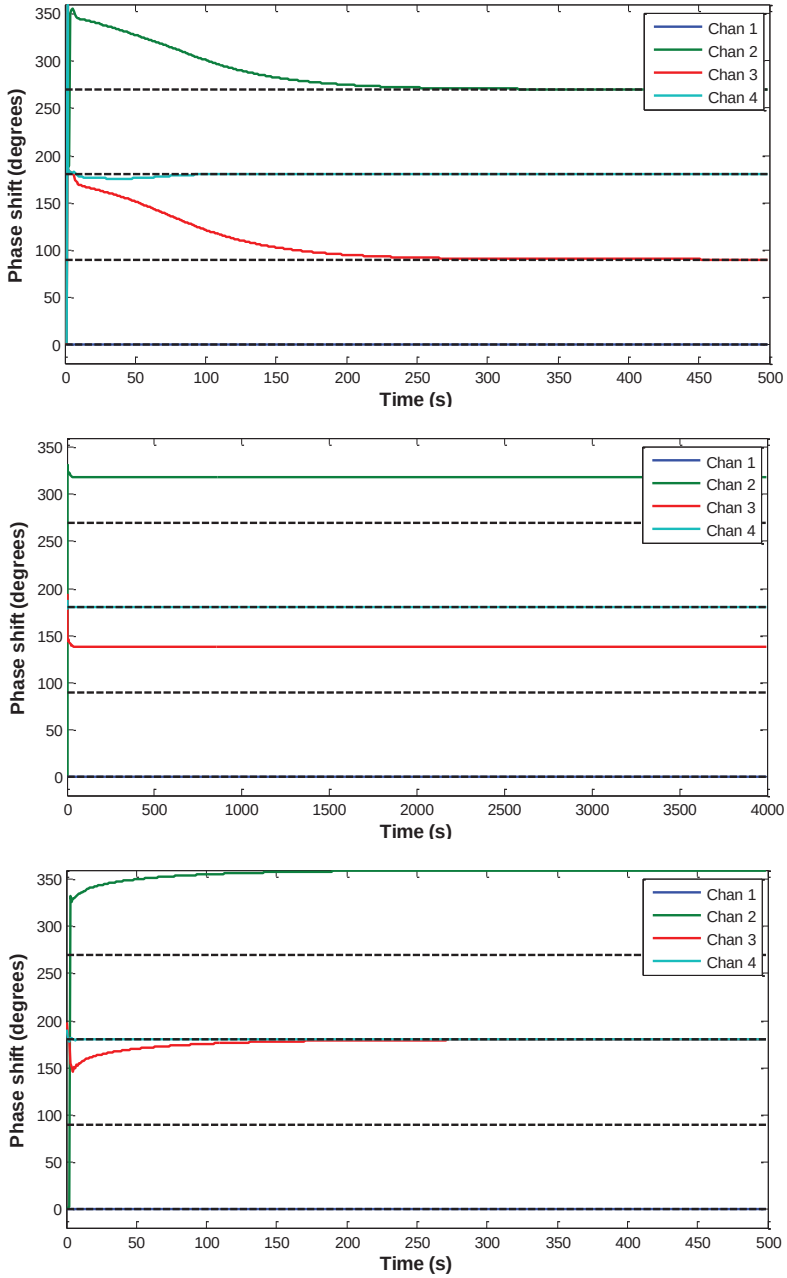

Figure 7. Evolution over time of the phase shift of each channel relative to Channel 1, for the coupled four-channel cases C-4G (top), C-4E (middle), and C-4C (bottom).

The results show the following clear trend: cases with relatively stronger TH channel coupling favor the rotating mode behavior, while cases with relatively stronger neutronic channel coupling favor the side-to-side mode. An interesting "transition region" also exists in this model, in which the final, converged limit cycle behavior is established at some intermediate phase shift somewhere between rotating and side-to-side.

4. CONCLUSIONS

The current study has proven successful in demonstrating a preferred "rotating mode" behavior using a reduced-order model with four TH channels connected by a common inlet plenum. Furthermore, a physical explanation has been established for why this mode is preferred for nonlinear limit cycle oscillations, drawing upon the conclusion that the rotating mode minimizes the variation in the average (or total) inlet flow rate, hence yields the most unstable oscillation pattern when an inlet plenum loss factor is included in the model.

However, for coupled calculations with multimodal neutronic feedback, it was found that the neutronic coupling favors the side-to-side oscillation mode, as opposed to the TH channel coupling which was found to always favor the rotating mode; the relative strength of these respective coupling mechanisms, adjusted via input parameters, determined which mode was the overall preferred mode. A physical explanation for why the neutronic coupling appears to favor the side-to-side mode specifically, is left as a topic of further investigation.

5. REFERENCES

1. R. Miro, D. Ginestar, D. Hennig and G. Verdu, "On the regional oscillation phenomenon in BWR's," *Progress in Nuclear Energy,* vol. 36, no. 2, pp. 189-229, 2000.
2. F. Zinzani, C. Demaziere and C. Sunde, "Calculation of the eigenfunctions of the two-group neutron diffusion equation and application to modal decomposition of BWR instabilities," *Annals of Nuclear Energy,* vol. 35, pp. 2109-2125, 2008.
3. A. Wysocki, J. March-Leuba, A. Manera and T. Downar, "TRACE/PARCS analysis of out-of-phase power oscillations with a rotating line of symmetry," *Ann. of Nuc. Energy,* vol. 67, pp. 59-69, 2014.
4. A. Dokhane, H. Ferroukhi and A. Pautz, "On out-of-phase higher mode oscillations with rotation and oscillation of symmetry line using an advanced integral stability methodology," *Ann. Nuc. En.,* vol. 67, pp. 21-30, 2013.
5. S. Nakanishi, M. Ozawa and S. Ishigai, "The Modes of Flow Oscillation in Multi-Channel Two-Phase Flow Systems," in *Advances in Two-Phase Flow and Heat Transfer,* vol. II, S. Kakac and M. Ishii, Eds., Boston, Martinus Nijhoff Publishers, 1983, pp. 709-724.
6. A. A. Karve, Rizwan-uddin and J. J. Dorning, "Stability analysis of BWR nuclear coupled thermal-hydraulics using a simple model," *Nuc. Eng. and Des.,* vol. 177, pp. 155-177, 1997.
7. A. Dokhane, "BWR stability and bifurcation analysis using a novel reduced order model and the system code RAMONA," Lausanne, 2004.
8. G. M. Grandi and K. S. Smith, "BWR stability analysis with SIMULATE-3K," in *Proc. of International Conference on the New Frontiers of Nuclear Technology Safety and High Performance Computing (PHYSOR-2002),* Seoul, Korea, 2002.
9. A. Wysocki, "Investigation of limit-cycle behavior in BWRs with time-domain analysis," Ann Arbor, MI, 2015.